

# Deforming Rheological Objects Using an Adaptive Mesh

Huynh Quang Huy Viet, Takahiro Kamada, Hiromi T. Tanaka  
Computer Vision Laboratory, Department of Human and Computer Intelligence,  
College of Information Science & Engineering, Ritsumeikan University,  
Shiga, Japan.  
{viet, tkamada, hiromi}@cv.ci.ritsumei.ac.jp

Naoki Ueda  
Murata Manufacturing Co., Ltd, Japan.  
uedanaoki@cv.ci.ritsumei.ac.jp

## Abstract

The subject described herein is a novel method for modeling and visualizing the deformation of a rheological object. In the method, we propose a dynamic adaptive triangle mesh of which the vertex link is a rheology element consisting of the group of a viscous element joining to two viscous and elastic elements associated parallelly. Based on the physical and geometrical properties of a rheological object, the mesh conforms dynamically to the deformation. We apply the dynamic adaptive triangle mesh for the problems of visualizing force interactions of a deformation process.

**Keywords:** *rheological object, dynamic adaptive triangle mesh, deformation model, three-element mode, elastic element, viscous element.*

## 1 Introduction

Researches on models for simulating, rendering and visualizing the physical properties and the behaviors of deformable objects gives many important applications in medical imaging, computer graphics and artificial reality. The modeling of deformable objects have been studied since late 80's, starting by the works of Terzopoulos [[1], [2]]. In recent time, with demands arising from food process engineering on the simulations of the physical change of materials such as starch, meat, dough, tissue, organ in a manufacturing or handling process, it becomes essential to study deformable models of rheological objects [3].

Rheological objects are objects having both elasticity and viscosity properties; their flexible property can be expressed by a three-element model which is a group of a viscous element connecting two viscous and elastic elements associated parallelly as a substitute for the elastic element in the mass spring system. There are two unsolved problem arising in the researches: (i) what model can be build so as to efficiently express the behavior of a rheological objects; (ii) how to visualize the physical change such as: a strength or a weakness of interaction, the changing processes of the distributions of temperature, stiffness, chemi-

cal components, etc., inside a rheological object. The idea to deal with these problems is to utilize an adaptive mesh of which topology conforms in accord with the changing of rheological objects. There were very few research papers relating to this issue; in [[4], [5]] Lauchaud proposed a mesh of which topology structure is changed under the geometrical constraints, and applied the method for extracting objects from volumetric data with a coarse-to-fine approach. However, because of using the geometrical constraints, this method can not be applied for representing of the physical processes, generally.

In this article, we propose a dynamic adaptive triangle mesh of which the vertex link is a rheology element consisting of the group of a viscous element joining to two viscous and elastic elements associated parallelly. Based on the physical and geometrical properties of a rheological object, the mesh conforms dynamically to the deformation. We apply the dynamic adaptive triangle mesh for the problems of visualizing force interactions of a deformation process.

The remainder of the article is organized as follows: next section reviews the three element model in prior works. Section 3 shows a dynamic adaptive triangular mesh which conforms to the changing physical properties of a rheological object. Section 4 represent the procedure for modeling the deformation of a rheological object and visualization the force interactions. Section 5 describes experimental results and discussions. Finally, Sect. 6 is devoted for conclusions and future works.

## 2 Rheological Object

### 2.1 Characteristic of Rheological Objects

Rheological objects deform in response to applied external force. Suppose that an object has a natural shape, as shown in Fig. 1(a). Applying external force, the object deforms as shown in Fig. 1(b). After external force is removed, rheological objects do not return to the original shape; however, the deformed shape is partially restored, as shown in Fig. 1(e). This type of deformation is called

bouncing deformation. And, the remaining deformation is called residual deformation. Thus, the rheological object in Fig. 1(e) has three deformation properties follows: (1) Residual deformation is involved, (2) bouncing displacement is involved, (3) vibrations decrease.

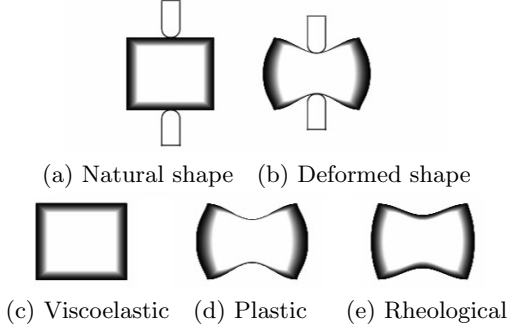


Figure 1: Rheological objects

## 2.2 Three-element model for the rheological object representation

We adopt the three-element model proposed to describe deformation characteristic of rheological objects [6]. In the three-element model, an elastic element and a viscous element are introduced to describe the time-dependent viscous and elastic deformation of a rheological object, as shown in Fig. 2. The relationship between deformation and force applied can be described by either serial or parallel combinations of these two fundamental elements, and these combinations are called rheology elements.

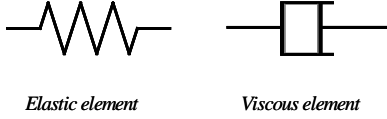


Figure 2: Fundamental elements

Rheology elements do not have bouncing deformation property if the residual deformation part has only the viscous element. Rheology elements have bouncing deformation property if either the non-residual deformation part or the residual deformation part has an elastic element. And, simple harmonic motion is generated in the deformation part if an elastic element exists independently. From the above discussion, the three-element model is obtained as a rheology element which consists of minimum number of fundamental elements, as shown in Fig. 3.

The three-element model is formulated as follows. Let  $P_i$  and  $P_j$  be two end points with the same mass  $m$  of the rheological element. Elastic and viscosity coefficients in the non-residual deformation part are denoted as  $k_1$  and  $c_1$  respectively. The other viscosity coefficient in the residual deformation part is denoted as  $c_2$ . The natural length of the non-residual deformation part is given by a  $r_0$ , and its

length in time is denoted by a function  $r_v(t)$ . The length of the rheological element in time is denoted by a function  $r_{ij}(t)$ . Let  $\mathbf{x}_i(t)$ ,  $\mathbf{x}_j(t)$  and  $\mathbf{v}_i(t)$ ,  $\mathbf{v}_j(t)$  be the position and velocity vectors of the mass  $P_i$  and  $P_j$  in turn. The rheological element's length can be expressed the position vector as follows:

$$r_{ij}(t) = (\mathbf{x}_j(t) - \mathbf{x}_i(t)) \mathbf{e}_{ij}, \quad (1)$$

here, vector  $\mathbf{e}_{ij}$  is the unit vector in direction from  $P_i$  to  $P_j$ , which is given by  $\mathbf{e}_{ij} = (\mathbf{x}_j(t) - \mathbf{x}_i(t)) / |\mathbf{x}_j(t) - \mathbf{x}_i(t)|$

Let  $f_e(t)$  be a force acting on the mass point  $P_i$  exerted by the rheological element between  $P_i$  and  $P_j$ ; this force equals to force acting on the non-residual deformation part:

$$f_e(t) = -c_1 \dot{r}_v(t) - k_1 (r_v(t) - r_0), \quad (2)$$

Moreover,  $f_e$  also coincides with the force caused by the damper of the residual deformation part:

$$f_e(t) = -c_2 (\dot{r}_{ij}(t) - \dot{r}_v(t)). \quad (3)$$

From the equations (2) and (3), we have:

$$\dot{r}_v(t) = \frac{-k_1 (r_v(t) - r_0) + c_2 \dot{r}_{ij}(t)}{c_1 + c_2} \quad (4)$$

here, the quantity  $\dot{r}_{ij}(t)$  can be calculated from the expression of the element's length  $r_{ij}(t)$ :

$$\dot{r}_{ij}(t) = (\mathbf{v}_j(t) - \mathbf{v}_i(t)) \mathbf{e}_{ij} \quad (5)$$

The equation of Newton's second law for the mass  $P_i$  is as follows:

$$m \dot{\mathbf{v}}_i(t) = f_e(t) \mathbf{e}_{ij} + \mathbf{F}^{ext}(t), \quad (6)$$

here,  $\mathbf{F}^{ext}(t)$  is the vector of an external force.

The equations (4) and (6) describe the deformation of a three element model. By solving the equations (4) and (6) for  $r_{ij}(t)$  and  $r_v(t)$ , we have the deformation formulation.

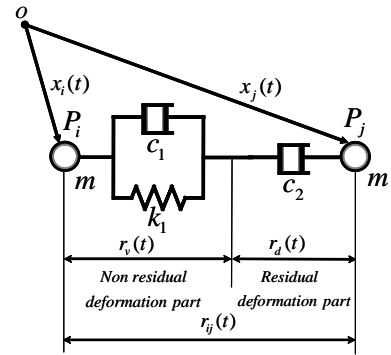


Figure 3: Three-element model

In next section, we show a dynamic adaptive triangular mesh of which the vertex connection is the three element model, for modeling the deformation of rheological object.

### 3 Adaptive Triangular Mesh Generation

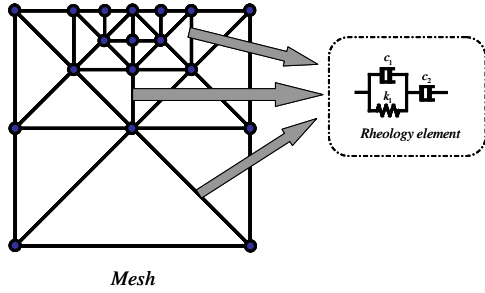


Figure 4: Dynamic adaptive triangular mesh

In the prior works, one of the authors proposed a method for generation of a adaptive mesh without cracks, and applied it for the problem of sampling and reconstructing range images [[7], [8]]; the method have also been developed to a 3D adaptive tetrahedral grid for modeling 3D objects [9]. In the present work, we develop a dynamic adaptive triangle mesh, abbreviated as DAT mesh, which conforms to the changing physical properties of a rheological object. DAT mesh is a type of discrete model constructed from physically-based vertexes, elastic elements and viscous elements as showed in Fig. 4; mesh elements are triangles which adapt to physical and geometrical problem under consideration, and dynamically grow smaller or bigger depending on the physical status of the vertexes. We implement the DAT mesh whose vertex links are rheology elements for modeling the deformation, visualizing the internal physical interactions, and rendering of cutting of a rheological object. The modeling of the deformation composes of two stages: (i) the stage of generating DAT mesh, (ii) the stage of representing the dynamic property. At first, we present the stage of DAT mesh generation.

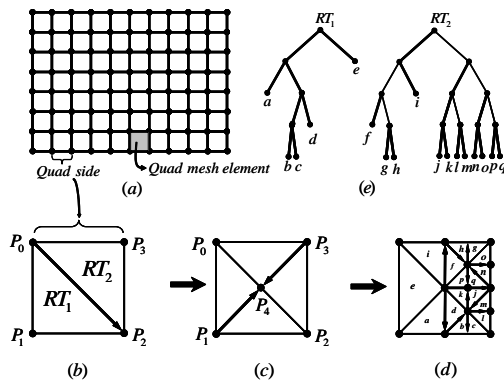


Figure 5: Adaptive Mesh Generation

To reduce the computation time for modeling the deformation, it is necessary to represent the object shape by a mesh of which elements are fine for the local area of limit

points being speculated such as boundaries or edges, and are rough otherwise. The aim of the mesh generation stage is to express the shape of a rheological object by a DAT mesh fitting to the shape boundary. For the sake of simplicity of modeling, the rheological object is supposed to have the shape of a rectangle, which is visualized by an image as showed in Fig. 5. The image is initially segmented into a set of regularly located square blocks with size of  $QuadSize^2$ , where each boundary of each quadrilateral mesh element is bounded and shared by its four adjacent mesh elements. Each mesh element is then segmented into two "root triangles" (Fig. 5b), so that the image becomes defined with a set of triangular blocks (hereon, we call simply "triangle" as the block enclosed with an isosceles right triangle). Then, the binary division process starts at all root triangles. According to the local geometry properties, the root triangles are bisected recursively and independently; this splitting process is repeated until all the resultant blocks satisfy the given criteria in order that fine meshes element are generated at the boundary (Fig. 5(c), (d)). As a result of this, the parent triangles are split into a hierarchical sets of triangles which would be represented as a binary tree, we call "split tree". An example of a split tree is shown in Fig. 5(e). Figure 6 gives the representation of an object using adaptive mesh.

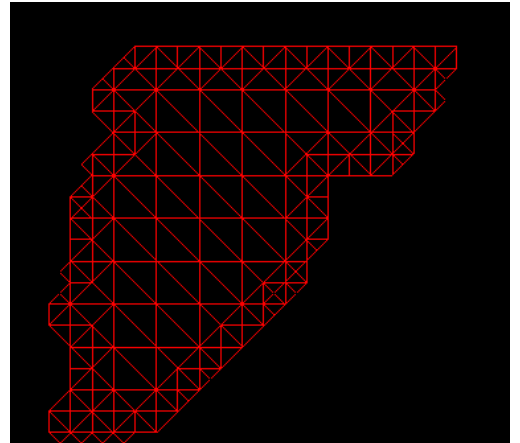


Figure 6: Representation of an object (shape of the liver) using adaptive mesh

### 4 Simulation Procedure of the Deformation Process

After the stage of generating the DAT mesh of a rheological object, the modeling of the deformation process under an external force is carried out by the procedure as shown in Fig. 7. The deformation can be modeled via dynamics equations of masses, viscous elements and elastic elements of the DAT mesh. Let  $S_h$  be a sets of element  $E_h$  applying their forces to a mass  $P_i$ , and Let  $S_j$  be a sets of elements  $E_j$  applied by the force of the mass  $P_i$ . Then, the total forces acting on  $P_i$  from all elements in two sets  $S_h$  and

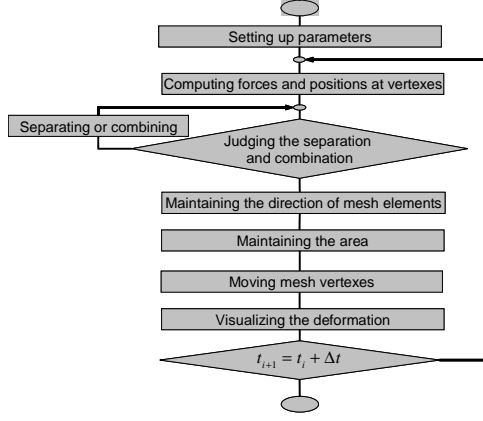


Figure 7: The simulation procedure flowchart

$S_j$  in union with external forces  $F_i^{ext}$  can be described as follows:

$$M\dot{\mathbf{v}}_i = \sum_{h \in S_h} f_h e_{hi} - \sum_{j \in S_j} f_j e_{ij} + F_i^{ext}. \quad (7)$$

Note that the equation (7) is the equation (6) applied for rheological elements in the DAT mesh. By solving the equations(2), (3) and (7) by use of a numerical method, such as Euler or Runge-Kutta, we can compute the deformation of a rheological object.

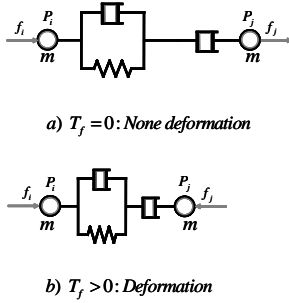


Figure 8: Subdivision Criterion

For the aim of visualization the behavior of internal forces acting within a rheological, after each step  $\Delta t$  for computing the position and the force on vertexes, the separation or combination of mesh elements is performed basing on the ratio of magnitude of difference force vectors and length of vertexes as expressed in the following expression:

$$T_f = \frac{|f_i - f_j|}{r_{ij}}, \quad (8)$$

here,  $r_{ij}$  is the length of an edge  $P_i P_j$  of a triangular element in the DAT mesh. The expression (9) is a criterion for the separation or combination judgment;  $T_f$  stands for the largeness of forces on a unit length, deforming the rheological element between two masses at the vertexes (see

Fig. 8);  $T_f$  becomes null when the total forces acting on  $P_i$  is identical the total forces acting on  $P_j$  (suppose that  $P_i$  and  $P_j$  have the same mass), in other words, when the rheological element is not deformed. In order avoiding the influence of the mass element in subdivision processes, the following criterion is utilized instead:

$$T_a = \frac{|\dot{\mathbf{v}}_i - \dot{\mathbf{v}}_j|}{r_{ij}}, \quad (9)$$

here,  $\dot{\mathbf{v}}_i$  and  $\dot{\mathbf{v}}_j$  are acceleration vectors of masses  $P_i$  and  $P_j$ . If the acceleration of a masses in an edges reaches a criterion for subdivision  $T_a^{sub}$ , the triangle is subdivided by a procedure similar to the triangle subdivision presented in the previous section. With the passing time, the acceleration of masses have tendency to decrease to zero; on the edges of subdivided triangles, when they encounter a criterion for combination  $T_a^{comb} (< T_a^{sub})$ , combination processes will happen. Figure 9 gives an illustration of the separation or combination procedure.

The mass of vertexes  $P_i$  in new triangles is computed basing on the mass density of the rheological object before deformation as follows:

$$m_i = \frac{M}{S} \sum_k \frac{S_{ik}}{3} \quad (10)$$

here,  $M$  and  $S$  are total mass and area of a rheological object;  $S_{ik}$  is the areas of the triangles which share the same vertex  $P_i$ . For instance, as shown in Fig. 9(a), the masses of vertexes  $P_i, P_h$  are  $\frac{M}{S} (\frac{S_1}{3} + \frac{S_2}{3})$ , that of vertexes  $P_j$  and  $P_k$  are  $\frac{M}{S} \frac{S_1}{3}$  and  $\frac{M}{S} \frac{S_2}{3}$  in turn.

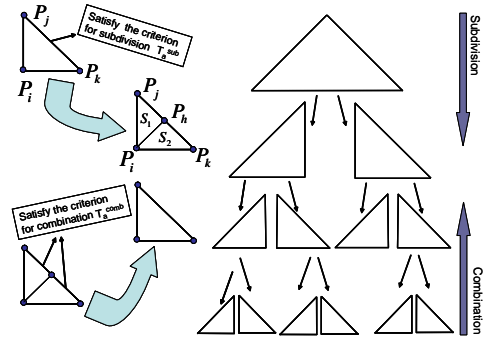


Figure 9: Subdivision and combination process

From time to time, the computing the position of vertexes at each step gives one of two unexpected results such as: (1) the mesh element is deformed reflectively, and (2) the length of rheological element is shorter than the length of a non-residual part, resulting in failure of the simulation. We refer [10] to deal with this problem.

For restraining a triangle mesh element  $\Delta P_i P_j P_k$  from the reflective deformation, we define the artificial force generated by a virtual Voigt model on the edges; e.g. the force on  $P_i P_j$  is formulated as follows:

$$\mathbf{f}_{ij}^k = \begin{cases} 0 & (d_{ij}^k > \epsilon) \\ (-K(d_{ij}^k - Cd_{ij}^k)) & (d_{ij}^k \leq \epsilon) \end{cases}, \quad (11)$$

here,  $d_{ij}^k$  is a distance from vertex  $P_k$  to edge  $P_iP_j$  (refer Fig. 10);  $K$  and  $C$  are the parameters of the Voigt model; and  $\epsilon$  is a small positive threshold value. When the distance  $d_{ij}^k$  becomes smaller than the threshold value  $\epsilon$ , the artificial force is applied to  $P_k$  to increase the signed distance.

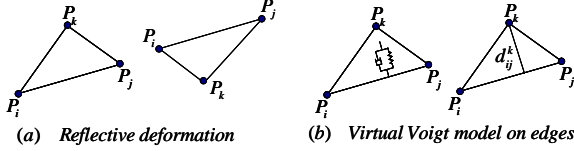


Figure 10: Reflective deformation and virtual Voigt model

For restraining the lengths of a non-residual part and a rheological element, we define the ratio  $a = r_v/r_{ij}$ , and assign it a possible value interval  $(a_{min}, a_{max})$ . That is to say, the ratio  $a$  of the length of a Voigt part and that of a rheological element is required to satisfy the following constrain:

$$a_{min} \leq a \leq a_{max}. \quad (12)$$

During the computation process, when the Voigt part length becomes smaller than  $a_{min}r_{ij}$ , it is assigned the minimum value  $a_{min}r_{ij}$ ; otherwise, when becoming greater than  $a_{max}r_{ij}$ , it is assigned by  $a_{max}r_{ij}$  itself.

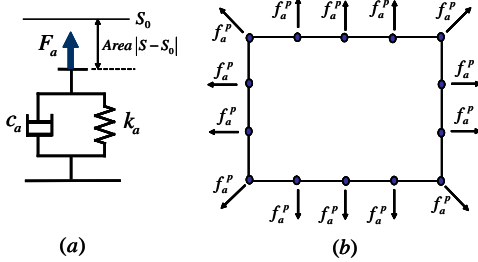


Figure 11: Area element

It is true that the volume of a rheological object is closely unchanged in a deformation process [3]. This means that, during 2D deformation simulation, the area of a rheological object must be preserved. For this reason, after each step of computing vertex positions, we reassign the force acting on vertexes of the boundary, basing on the area element defined by the Voigt model for an area, as shown in Fig. 11. The force acting on area element is formulated as follows:

$$F_a = -k_a(S - S_{int}) - c_a\dot{S} \quad (13)$$

here,  $S_{int}$  is the initial area of the rheological object;  $k_a$  and  $c_a$  are the parameters of the Voigt model. The constrain forge on each vertex  $P_i$  of the boundary can be computed by the following expression:

$$f_i^p = \frac{r_{hi}F_a}{2L} + \frac{r_{ij}F_a}{2L} \quad (14)$$

here,  $r_{hi}$  and  $r_{ij}$  are the lengths of the two rheology elements on the boundary sharing the vertex  $P_i$ ; and  $L$  is the boundary length.

After maintaining the area for the subsequent loop of computing, the next step in the procedure is to move vertexes and visualize the deformation (see Fig. 7). In the experimental results section, we show the effectiveness of the proposed method.

## 5 Experimental Results

For evaluating the method, we construct a system for measurement of the displacement height of dough (a rheological object) under pressure. Figure 12 shows the measurement system. The result of measuring the deformation of dough and the result of the simulation on deformation of a rheological object are plotted in Fig. 13. The deformation process is divided into three phrase at time  $T_c$  of contact, at time  $T_s$  of maximum displacement height reached, and at  $T_e$  of contact force released.

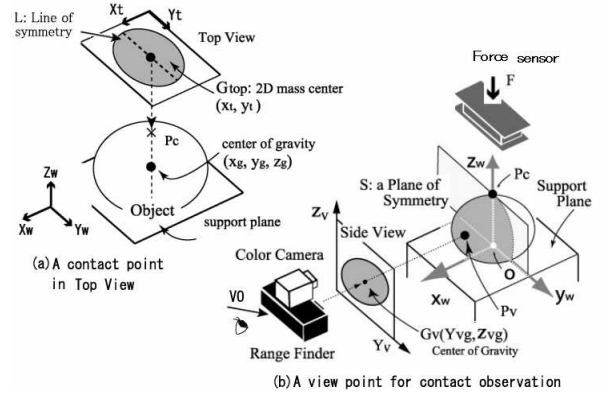


Figure 12: System for measurement of the deformation of dough

The simulation of the deformation of a rheological object is performed as presented in Sect.4. The displacement height of the contact point is plotted in an appropriate scale for comparison. In Fig. 13, the height and shape of the simulated rheological object do not restore to their initial statuses; although in phrase 3, the displacement of the simulated result is greater than the measured displacement, the forms of the curves are likely the same in general. Besides, the subdivision and combination of the triangles in the phrases of the deformation process displays visually the force interaction. These show the effectiveness of the proposed method for modeling and visualization.

The experiment is also extended on simulating the deformation of a viscoelastic object (by substituting the damper parameter in rheology elements of mesh by zeros), on measuring the deformation of a spring (having the viscoelastic property). Figure 14 shows the result; the perfect restoration of the shape and the coincidence of the simulated result with the measured result prove the correctness of the proposed method.

## 6 Conclusions

We have described a new method for 2D modeling and visualizing the deformation process of a rheological object. The experimental results showed the effectiveness of the proposed method. The future works are addressed on extending the proposed method for 3D modeling.

## References

- [1] D. Terzopoulos, J. Platt, A. Barr and K. Fleischer: “Elastically deformable models”, *Computer Graphics (Proc. SIGGRAPH’87)*, **21**, 4, pp. 205–214 (1987).
- [2] D. Terzopoulos and K. Fleischer: “Modeling inelastic deformation: Viscoelasticity, plasticity, fracture”, *Computer Graphics (Proc. SIGGRAPH’88)*, **22**, 4, pp. 269–278 (1988).
- [3] N. Ueda, S. Hirai and H. Tanaka: “Extracting rheological properties of deformable objects with haptic vision”, *Proc. IEEE Int. Conf. on Robotics and Automation*, New Orleans, pp. 3902–3907 (2004).
- [4] J. Lachaud and A. Montanver: “Deformable meshes with automated topology changes for coarse-to-fine 3d surface extraction”, *Medical Image Analysis*, **3**, 2, pp. 187–207 (1999).
- [5] J. Lachaud and B. Taton: “Deformable model with adaptive mesh and automated topology changes”, *Proc. Fourth Int. Conf. 3-D Digital Imaging and Modeling (3DIM’2003)*, Banff, Alberta, Canada, pp. 12–19 (2003).
- [6] S. Tokumoto, S. Hirai and H. Tanaka: “Constructing virtual rheological objects”, *Proc. Fifth World Multiconference on Systemics, Cybernetics and Infomatics (SCI 2001)*, Orlando, Florida, USA, pp. 106–111 (2001).
- [7] H. T. Tanaka and F. Kishino: “Adaptive mesh generation for surface reconstruction: Parallel hierarchical triangulation without discontinuities”, *Proc. IEEE Conf. Computer Vision Pattern Recognition (CVPR93)*, New York City, pp. 88–94 (1993).
- [8] H. T. Tanaka: “Accuracy-based sampling and reconstruction with adaptive meshes for parallel hierarchical triangulation”, *Computer Vision and Image Understanding*, **61**, 3, pp. 335–350 (1995).
- [9] H. T. Tanaka, Y. Takama and H. Wakabayashi: “Accuracy-based sampling and reconstruction with adaptive grid for parallel hierarchical tetrahedrization”, *Proc. the 2003 Eurographics/IEEE TVCG Workshop on Volume graphics*, Tokyo, Japan, pp. 79–86 (2003).
- [10] M. Kimura, Y. Sugiyama, S. Tomokuni and S. Hirai: “Deformation simulation in virtual rheological objects”, *Proc. of the 7th Virtual Reality Society of Japan Annual Conference*, Tokyo, Japan (2002).
- [11] H. Delingette: “General object reconstruction based on simplex meshes”, *International Journal of Computer Vision*, **32**, 2, pp. 111–146 (1999).
- [12] T. McInerney and D. Terzopoulos: “Medical image segmentation using topologically adaptable surfaces”, *Proc. the First Joint Conference on Computer Vision, Virtual Reality and Robotics in Medicine and Medial Robotics and Computer-Assisted Surgery (CVRMed-MRCAS’97)*, Grenoble, France, pp. 23–32 (1997).
- [13] T. McInerney and D. Terzopoulos: “Deformable models in medical image analysis: A survey”, *Medical Image Analysis*, **1**, 2, pp. 91–108 (1996).
- [14] C. Mendoza and C. Laugier: “Simulating soft tissue cutting using finite element models”, *Proc. of the IEEE Int. Conf. on Robotics and Automation*, Taipei, Taiwan, pp. 1109–1114 (2003).
- [15] S. Miyazaki, M. Endo, M. Yamada and J. Hasegawa: “A deformable fast computation elastic model based on element reduction and reconstruction”, *Proc. 2004 Int. Conf. on Cyber Worlds (CW2004)*, Tokyo, Japan, pp. 94–99 (2004).
- [16] J. Montagnat, H. Delingette and N. Ayache: “A review of deformable surfaces: topology, geometry and deformation”, *Image and Vision Computing*, **19**, 14, pp. 1023–1040 (2001).
- [17] H. Nienhuys and A. Stappen: “A surgery simulation supporting cuts and finite element deformation”, *Proc. Fourth Int. Conf. on Med. Image Comput. and Computer-Assisted Intervention (MICCAI 2001)*, Utrecht, The Netherlands, pp. 145–152 (2001).
- [18] H. Nienhuys and A. Stappen: “Supporting cuts and finite element deformation in interactive surgery simulation”, *Technical Report UU-CS-2001-16*, Utrecht University, Institute of Information and Computing Sciences, PO Box 80.089, 3508 TB, The Netherlands (2001).
- [19] A. Tanaka, K. Hirota and T. Kaneko: “Deforming and cutting operation with force sensation”, *Journal of Robotics and Mechatronics*, **12**, 3, pp. 292–303 (2000).

## About the authors

Huynh Quang Huy Viet is currently a postdoctoral fellow at Department of Human and Computer Intelligence, College of Information Science & Engineering, Ritsumeikan University, Japan.

Takahiro Kamada is a student in Master course of Department of Human and Computer Intelligence, College of Information Science & Engineering, Ritsumeikan University, Japan.

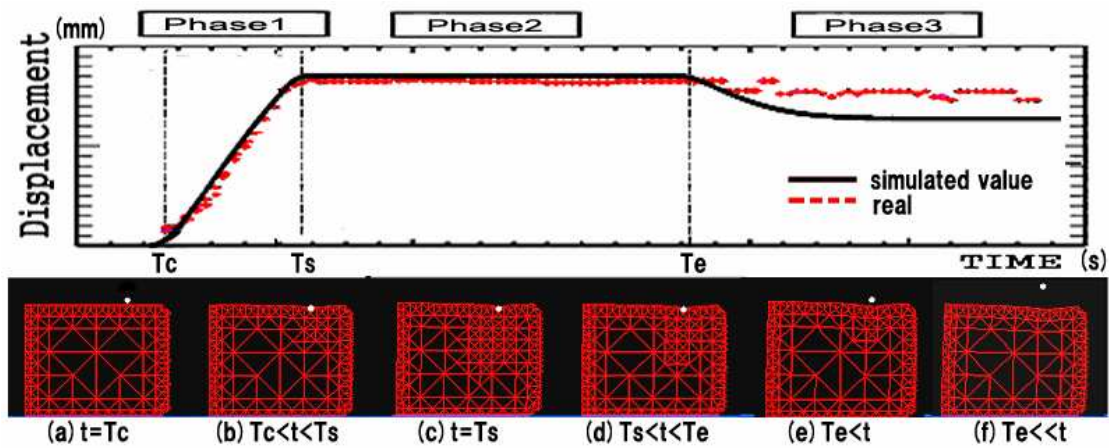


Figure 13: Measured and simulated results of the deformation of a rheological object

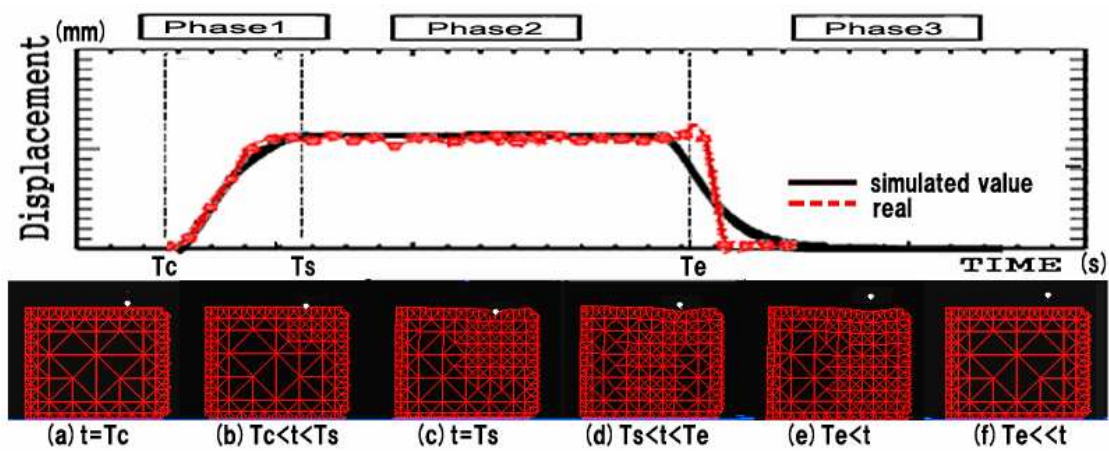


Figure 14: Measured and simulated results of deformation of a viscoelastic object

Naoki Ueda currently works at Murata Manufacturing Co., Ltd, Japan.

Hiromi T.Tanaka is a professor at Department of Human and Computer Intelligence, College of Information Science & Engineering, Ritsumeikan University, Japan.